# Synthesis and In Vivo Evaluation of $^{18}$F-Desbromo-DuP-697 as a PET Tracer for Cyclooxygenase-2 Expression

Erik F.J. de Vries, PhD; Aren van Waarde, PhD; Anne Rixt Buursma, MSc; and Willem Vaalburg, PhD

*PET Center, Groningen University Hospital, Groningen, The Netherlands*

Cyclooxygenase-2 (COX-2) overexpression has been observed in various pathologies, such as inflammation, cancer, ischemia, and Alzheimer's disease. As an initial step toward a noninvasive PET technique to assay COX-2 expression, this study describes the synthesis and preliminary evaluation of the radiolabeled COX-2 inhibitor $^{18}$F-desbromo-DuP-697. **Methods:** Desbromo-DuP-697 was radiolabeled by a nucleophilic aromatic substitution reaction of the nitro precursor with $^{18}$F-fluoride. Biodistribution studies of the tracer were performed in a carrageenan-induced hyperalgesia rat model. Brain uptake was investigated with autoradiography. To confirm the results of the biodistribution, COX activity was determined by a peroxidase assay. **Results:** Biodistribution studies showed specific binding of the tracer to COX-2 in heart, kidney, brain, and blood cells, but not in the inflamed paw, which was probably due to low COX-2 expression. In the brain, regional differences in tracer uptake were observed, with high uptake in cortical regions. $^{18}$F-Desbromo-DuP-697 did not show any binding to COX-1. Nonspecific uptake was high in fat and intestines. **Conclusion:** Because of its ability to cross the blood–brain barrier, $^{18}$F-desbromo-DuP-697 appears to be suitable for COX-2 imaging in the brain. Its high nonspecific uptake in the intestines may limit its use for imaging in the abdominal region.

**Key Words:** PET; desbromo-DuP-697; cyclooxygenase-2; inflammation; carrageenan

**J Nucl Med 2003; 44:1700–1706**

Cyclooxygenase (COX) is an essential enzyme in the biosynthesis of prostaglandins and thromboxanes. Thus far, 2 isoforms of the enzyme have been discovered. COX-1 is constitutively expressed in most tissues, functions as a housekeeping enzyme, and is responsible for the normal production of eicosanes. COX-2 is predominantly found in brain and kidneys and is virtually absent in most other tissues. However, COX-2 expression can be transiently induced by inflammatory stimuli. Nonsteroidal antiinflammatory drugs (NSAIDs), such as aspirin and indomethacin, can inhibit COX activity and have frequently been used in the treatment inflammatory diseases like arthritis (*1*). The most common side effects of the first-generation NSAIDs are platelet aggregation, gastrointestinal erosion, and bleeding. The adverse effects of NSAIDs were ascribed to inhibition of COX-1, whereas the antiinflammatory properties of NSAIDs were attributed to inhibition of COX-2. This has prompted researchers to develop novel NSAIDs that were highly selective for COX-2.

In the last decade, increasing evidence has shown that COX-2 is not only implicated in inflammation but also in various other pathologic processes (*2*). For example, in a variety of tumors, such as colorectal, gastric, and breast tumors, overexpression of COX-2 is observed (*3*). COX-2 is thought to play an important role in carcinogenesis by stimulating angiogenesis, tissue invasion, and metastasis and by inhibiting apoptosis (*4*). COX-2 is also overexpressed in cardiac and cerebral ischemic tissue and is responsible for the late-phase injury (*5*,*6*). Several studies indicate that COX-2 is also involved in neurodegenerative diseases, like Alzheimer's and Parkinson's, in which COX-2 overexpression may induce neuronal degeneration (*7*).

In general, COX-2 expression in humans is assessed by ex vivo laboratory analysis of invasively acquired or postmortem tissue samples. Because COX-2 messenger RNA (mRNA) and protein are highly unstable (half-life, 1–3.5 h), the results of ex vivo COX-2 analysis strongly depend on the interval between tissue sampling or time of death and analysis (*8*,*9*). A noninvasive imaging method to monitor COX-2 expression could overcome this complication and may provide a valuable tool to gain more insight in the role of COX-2 in pathologic processes, especially in neurologic disorders in which repetitive tissue sampling is not possible. A noninvasive imaging technique, such as PET, could also be applied in the in vivo evaluation of novel selective COX-2 inhibitors and in dose-escalation studies. This information can be of great value, because assessment of the clinical relevance of COX inhibitors by extrapolating in vitro data alone is usually inaccurate (*10*).

Received Feb. 19, 2003; revision accepted Jun. 13, 2003.

For correspondence contact: Erik F.J. de Vries, PhD, PET Center, Groningen University Hospital, P.O. Box 30,001, 9700 RB Groningen, The Netherlands.

E-mail: e.f.j.de.vries@pet.azg.nl

Recently, the selective COX-2 inhibitor SC-58125 was labeled with $^{18}F$ and evaluated as a tracer for PET imaging (*11*). In vitro, encouraging results were obtained, as $^{18}F$-SC-58125 showed enhanced uptake in stimulated macrophages, which could be reduced to basal levels by the addition of carrier SC-58125. However, specific binding to COX-2 could not be demonstrated in vivo, because there was no blocking of tracer uptake by carrier SC-58125. In monkey brain, no regional differences in the distribution of $^{18}F$-SC-58125 could be found.

We have focused on another COX-2 inhibitor, DuP-697 (compound 1). DuP-697 is a very potent and selective irreversible COX-2 inhibitor (*12*), which is not metabolized in humans (*13*). In a previous study, we attempted to label DuP-697 via an $^{18}F$ for $^{19}F$ exchange reaction (Fig. 1). Instead of $^{18}F$-DuP-697, its carrier-added desbromo derivative (compound 2) was formed (*14*). Literature data, however, suggest that radiolabeled desbromo-DuP-697 might also be a suitable PET tracer for imaging COX-2 expression. In vitro studies have shown that desbromo-DuP-697 has a high affinity and is even more selective for COX-2 than DuP-697 (*15,16*).

In this study, a labeling procedure for noncarrier-added $^{18}F$-desbromo-DuP-697 is described. This $^{18}F$-labeled COX-2 inhibitor was evaluated in a rat model for carrageenan-induced hyperalgesia. In this model, injection of a carrageenan solution induces sterile inflammation in the rat paw. Maximum upregulation of COX-2 mRNA and protein levels in the inflamed paw were already observed within 1 h after carrageenan injection (*17*).

## MATERIALS AND METHODS

All chemicals were commercially available and used without further purification, except for 3-[4-(methylthio)phenyl]-2-(4-nitrophenyl)thiophene (compound 3), which was prepared as described by Tsuji et al. (*18*). $^1H$ nuclear magnetic resonance (NMR) (200 MHz) and $^{19}F$ NMR (188 MHz) spectra were recorded on a Varian Gemini 200 spectrometer. $^1H$ chemical shifts were determined relative to the signal of the solvent, converted to the tetramethylsilane scale and expressed in δ units (parts per million) downfield from tetramethylsilane. $^{19}F$ chemical shifts were determined relative to the signal of $CClF_3$. Electrospray mass spectrometry (MS) was obtained in 80% acetonitrile with 0.1% formic acid using a Perkins Elmer Sciex API 3000 mass spectrometer. High-performance liquid chromatography (HPLC) analyses and preparative separations were performed on a Waters system, consisting of a 515 isocratic pump, a 486 multiwavelength ultraviolet detector operated at 254 nm, and a Bicron Geiger–Müller radioactivity detector. The COX inhibitors DuP-697, NS398, and indomethacin were purchased from Sigma Chemical Co.

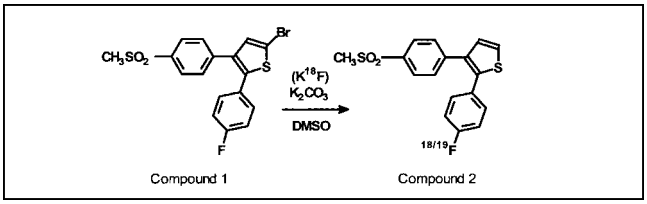


**FIGURE 1.** Attempted radiosynthesis of carrier-added DuP-697 (compound 1) via $^{18}F$ for $^{19}F$ exchange reaction, which resulted in formation of $^{18}F$-desbromo-DuP-697 (compound 2). DMSO = dimethyl sulfoxide.

### Chemistry

*2-(4-Fluorophenyl)-3-[4-(Methylsulfonyl)Phenyl]Thiophene (Compound 2).* A solution of 5 mg $K_2CO_3$ in 1 mL water was added to 20 mg Kryptofix 2.2.2. (Merck) in 1 mL acetonitrile. The solvents were evaporated at 130°C and the residue was dried 3 times with 0.5 mL acetonitrile. To the dried $K_2CO_3$/Kryptofix complex, a solution of 9.7 mg 5-bromo-2-(4-fluorophenyl)-3-[4-(methylsulfonyl)phenyl]thiophene (DuP-697, compound 1) in 0.5 mL dimethyl sulfoxide (DMSO) was added. The reaction mixture was allowed to react at 160°C for 30 min and subsequently cooled to room temperature. The reaction mixture was diluted with 2 mL water and passed through a Waters $C_{18}$ classic SepPak column. The SepPak was washed with 2 mL water and eluted with 5 mL acetonitrile. The eluate was concentrated in vacuo. The residue was dissolved in 1 mL ethyl acetate and passed through a Waters Silica Plus SepPak column. The SepPak was eluted with 5 mL ethyl acetate and the eluate was concentrated in vacuo. The residue was purified by preparative normal-phase HPLC using a Chrompak silica column (7.8 × 300 mm, 5 μm) and 25% ethyl acetate in hexane as the eluent (flow, 3 mL/min). The product with a retention time of 14 min was collected and concentrated in vacuo, yielding 4.0 mg (51%) desbromo-DuP-697 (compound 2) as a white solid. The product was characterized with NMR and MS. The analytic data are listed below. $^1H$ NMR (DMSO-$d_6$) δ: 7.85 (dt, 2H, $J$ = 8.5 Hz, $J$ = 2.0 Hz, Ph), 7.71 (d, 1H, $J$ = 5.1 Hz, thiophene), 7.48 (dt, 2H, $J$ = 8.5 Hz, $J$ = 2.0 Hz, Ph), 7.31 (d, 1H, $J$ = 5.1 Hz, thiophene), 7.29–7.15 (m, 4H, Ph), 3.21 (s, 3H, $CH_3$). $^{19}F$ NMR ($CDCl_3$) δ: −96.0. MS *m/z*: 333 (43%, M+1), 374 (25%, M+ACN+1), 665 (100%, 2M+1).

*2-(4-Nitrophenyl)-3-[4-(Methylsulfonyl)Phenyl]Thiophene (Compound 4).* 3-Chloroperbenzoic acid (370 mg, 70%–75%) was added to a solution of 160 mg (0.5 mmol) compound 3 (*18*) in 5 mL $CH_2Cl_2$. After the reaction mixture was stirred at ambient temperature for 18 h, the mixture was filtered. The filtrate was washed with 25 mL saturated $NaHCO_3$ solution. The water layer was extracted again with 25 mL $CH_2Cl_2$. The combined organic layers were dried on anhydrous $Na_2SO_4$ and concentrated in vacuo. The residue was purified by flash column chromatography (silica 60, eluent: ethyl acetate/hexane, 1:1), affording 130 mg (74%) desired product as a yellow solid. The product was characterized with NMR spectroscopy. The analytic data are listed below. $^1H$ NMR ($CDCl_3$) δ: 8.15 (dt, 2H, $J$ = 9.0 Hz, $J$ = 2.3 Hz, Ph), 7.89 (dt, 2H, $J$ = 8.6 Hz, $J$ = 2.0 Hz, Ph), 7.51 (d, 1H, $J$ = 5.2 Hz, thiophene), 7.45 (dt, 2H, $J$ = 8.6 Hz, $J$ = 2.0 Hz, Ph), 7.42 (dt, 2H, $J$ = 9.0 Hz, $J$ = 2.3 Hz, Ph), 7.20 (d, 1H, $J$ = 5.2 Hz, thiophene), 3.09 (s, 3H, $CH_3$).

### Radiochemistry: 2-(4-$^{18}F$-Fluorophenyl)-3-[4-(Methylsulfonyl)Phenyl]Thiophene (Compound $^{18}F$-2)

Aqueous $^{18}F$-fluoride was produced in a silver target with a Scanditronix MC-17 cyclotron via the $^{18}O(p,n)^{18}F$ nuclear reaction. The cyclotron-produced $^{18}F$-fluoride solution was passed through an AG1-X8 ion-exchange column ($CO_3^{2-}$ form) to recover the $^{18}O$-enriched water. The $^{18}F$-fluoride was eluted from the ion-exchange column with a solution of 1 mg $K_2CO_3$ in 1 mL water and collected in a vial with 15 mg Kryptofix 2.2.2. To this

solution, 1 mL acetonitrile was added and the solvents were evaporated at 130°C. The $K^{18}F$-F/Kryptofix complex was dried 3 times by the addition of 0.5 mL acetonitrile, followed by evaporation of the solvent. A solution of 1–2 mg compound 4 in 0.5 mL dry *N*,*N*-dimethylformamide was added to the dry $K^{18}F$-F/Kryptofix complex. The reaction mixture was heated to 160°C for 15 min and subsequently cooled in an ice bath for 2 min. The reaction mixture was diluted with 2.5 mL water and passed through a Waters $C_{18}$ classic SepPak column. The SepPak was washed with 2 mL water and eluted with 3 mL acetonitrile. The eluate was concentrated at 130°C with the aid of an argon flow. The residue was dissolved in 0.3 mL ethyl acetate, diluted with 0.7 mL hexane, and purified by normal-phase HPLC over a μPoracil silica column (7.8 × 300 mm, 5 μm) (Waters Chromatography) using 25% ethyl acetate in hexane as the eluent with a flow of 3 mL/min. The desired product (retention time, 14 min) was collected and the HPLC eluent was evaporated at 130°C with the aid of an argon flow. The product was obtained in 2.6% ± 1.6% ($n$ = 15) decay-corrected yield in approximately 70-min total synthesis time. A sample of the product was taken for quality control by reverse-phase HPLC on a μBondapak $C_{18}$ column (3.9 × 300 mm, 10 μm) (Waters Chromatography), using 50% aqueous acetonitrile as the eluent (flow, 1 mL/min). The product coeluted with an unlabeled reference sample. $^{18}$F-Desbromo-DuP-697 had a specific activity of 21–47 GBq/μmol and a radiochemical purity of >99%.

### Octanol–Water Partition Coefficient

To determine the lipophilicity of desbromo-DuP-697, 10 MBq of compound $^{18}$F-2 in a mixture of 5 mL octanol and 5 mL phosphate-buffered saline (PBS) at pH 7.4 were vigorously shaken for 30 min in a water bath at 37°C. After the layers were separated, a 25-μL sample of the organic layer and a 1-mL sample of the water layer were taken and the radioactivity was measured with a gamma counter. In 5 independent measurements, the average octanol–water partition coefficient, expressed as logP, was 3.72 ± 0.16. The calculated logP was 4.24 (CompuDrug Chemistry Ltd.).

### Biodistribution Studies of $^{18}$F-Desbromo-DuP-697

All studies were performed in compliance with the national law on animal experiments. The protocols were approved by the Animal Ethics Committee of the Groningen University.

The biodistribution of $^{18}$F-desbromo-DuP-697 was determined in the carrageenan-induced hyperalgesia model described by Nantel et al. (*17*). Male Sprague–Dawley rats (190–266 g) were anesthetized by intraperitoneal injection of a mixture of ketamine (25 mg/kg) and medetomidine (0.2 mg/kg). Hyperalgesia was induced by intraplantar injection of 150 μL of 3% carrageenan solution in PBS in the right hind paw of the anesthetized animal. This resulted in severe swelling of the carrageenan-injected paw. After 55 min, 0.3 mL NS-398 (1.5 mg/kg) in 96% ethanol/0.9% NaCl/propylene glycol (3:1:1), indomethacin (1.5 mg/kg) in PBS, or PBS alone was injected in the tail vein. One hour after the administration of carrageenan, 15–20 MBq $^{18}$F-desbromo-DuP-697 in a cocktail of 96% alcohol/0.9% NaCl/propylene glycol (1:2:2) were administered via injection into the tail vein. After 2 h of tracer distribution, the animals were killed by extirpation of the heart. Relevant tissues were dissected and weighed. Tracer uptake in the tissues was measured using a gamma counter and expressed as standardized uptake value (SUV), which was defined as:

$$\text{SUV} = \frac{\text{Tissue Activity Concentration}\left(\frac{\text{MBq}}{\text{g}}\right) \times \text{Body Weight (g)}}{\text{Injected Dose (MBq)}}.$$

### Autoradiography of Brain Slices

After 2 h of $^{18}$F-desbromo-DuP-697 distribution, isolated rat brains were frozen in liquid nitrogen and stored on dry ice. The frozen brain samples were cut into 80-μm-thick slices using a microtome at −6°C. Brain slices were placed on slides and covered with a multipurpose Cyclone Storage Phosphor Screen (Packard Instruments). After exposure for 24 h, the phosphor screens were scanned using a Cyclone imaging system (Packard Instruments).

### COX Peroxidase Assay

Peroxidase activity was assayed by measuring the COX-catalyzed oxidation of *N*,*N*,*N*′,*N*′-tetramethylphenylenediamine (TMPD) by hydrogen peroxide, according to the method described by van der Ouderaa and Buytenhek (*19*). Male Sprague–Dawley rats were anesthetized with a mixture of ketamine (25 mg/kg) and medetomidine (0.2 mg/kg) and injected with 150 μL of 3% carrageenan in PBS into the right hind paw. After 1 h, animals were killed by extirpation of the heart. Brain, heart, kidney, liver, lung, the inflamed paw, and a control paw were dissected, kept on ice, and immediately assayed. The tissues were weighed, cut into small pieces, and homogenized in 4 mL of 5 mmol/L ethylenediaminetetraacetic acid in 50 mmol/L Tris buffer at pH 8.0. The homogenates were centrifuged at 5,400 rpm for 10 min. At 21°C ± 1°C, 10 μL of supernatant were added to a quartz cuvette with 1.8 mL of 0.1 mol/L Tris buffer at pH 8.0, 5 μL of 1 μmol/L hemin solution in Tris buffer, and 100 μL of 2.4 mol/L aqueous TMPD. The assay was started by the addition of 100 μL of 9 mmol/L aqueous hydrogen peroxide to the cuvette. The oxidation of TMPD was monitored by measuring the absorption of the mixture with a spectrophotometer at 610 nm for 10 min. The initial oxidation rates (in absorption units per minute per gram of tissue) were determined from the absorption curves. In an identical manner, a calibration curve was made, using solutions of commercially available COX-2 (25–2,260 units/mL) instead of the tissue homogenates. The assay was linear with respect to COX-2 peroxidase activity within the concentration range that was used in this study. With the aid of the calibration curve, the tissue peroxidase activity could be expressed as COX-2 unit equivalents per gram of tissue.

## RESULTS

### Radiochemistry

The selective COX-2 inhibitor desbromo-DuP-697 (compound 2) was labeled with $^{18}$F via a nucleophilic substitution reaction on the corresponding nitro precursor (compound 4; Fig. 2). At 160°C, radiochemical yields of 2.6% ± 1.6% (corrected for decay) were obtained ($n$ = 15). Radiochemically pure (>99%) $^{18}$F-desbromo-DuP-697 with a specific activity of at least 20 GBq/μmol was prepared in approximately 70-min synthesis time. Desbromo-DuP-697 is a lipophilic compound with a logP of 3.7, which allows the tracer to cross the blood–brain barrier.

### Tracer Distribution

In vivo evaluation of compound $^{18}$F-2 was performed in a carrageenan-induced hyperalgesia model in adult

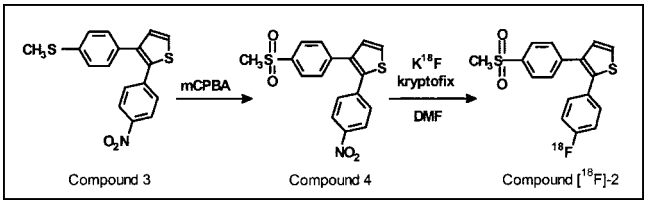


**FIGURE 2.** Preparation of radiopharmaceutical precursor (compound 4) from compound 3 (*18*), followed by labeling of noncarrier-added $^{18}$F-desbromo-DuP-697 (compound $^{18}$F-2). mCPBA = 3-chloroperbenzoic acid; DMF = *N,N*-dimethylformamide.

Sprague–Dawley rats. Two hours after intravenous injection of compound $^{18}$F-2, tracer distribution was determined in untreated control animals and in animals pretreated with either the selective COX-2 inhibitor NS-398 or the nonselective COX inhibitor indomethacin. The results, presented in Table 1, show that similar tracer uptake was observed in the inflamed and the control paw. Neither NS-398 nor indomethacin could reduce the tracer uptake in the inflamed paw, despite the fact that severe swelling of this paw was observed. The highest tracer uptake was found in the intestines and in fat, which could not be significantly reduced by treatment with COX inhibitors. The uptake of radioactivity in bone tissue was low, indicating that defluorination of the tracer was negligible. Pretreatment with the selective COX-2 inhibitor NS-398 significantly ($P < 0.05$) blocked tracer accumulation in heart (−60%), kidney (−46%), brain (−40%), and the cellular fraction of blood (−16%). The autoradiograms of brain slices of untreated rats showed regional differences in tracer uptake, with high uptake in most cortical areas (Fig. 3). In the brain of rats pretreated with NS-398, these regional differences were strongly suppressed. Administration of the nonselective COX inhibitor indomethacin before tracer injection had an effect on tissue uptake of compound $^{18}$F-2 similar to that of treatment with NS-398. Compared with control animals, animals pretreated with indomethacin showed significantly ($P < 0.05$) reduced tracer accumulation in heart (−61%), kidney (−52%), brain (−40%), spleen (−36%), and the cellular fraction of blood (−57%). The highest reduction in tracer uptake after pretreatment with NS-398 (−71%) or indomethacin (−75%) was observed in the lung. For both inhibitors, however, this reduction was not statistically significant ($P = 0.09$ and 0.08), mainly due to a wide variation in the tracer uptake in the lung of untreated control rats.

**TABLE 1**
Tissue Distribution of $^{18}$F-Desbromo-DuP-697 in Rats 120 Minutes After Tracer Injection

| Tissue | Control | NS-398 (1.5 mg/kg) | Indomethacin (1.5 mg/kg) |
|---|---|---|---|
| Blood cells | 0.08 ± 0.00 | 0.06 ± 0.01* | 0.03 ± 0.01† |
| Bone | 0.09 ± 0.02 | 0.10 ± 0.03 | 0.07 ± 0.01 |
| Cerebellum | 0.18 ± 0.01 | 0.10 ± 0.01† | 0.11 ± 0.03* |
| Cerebrum | 0.18 ± 0.03 | 0.11 ± 0.01* | 0.11 ± 0.03‡ |
| Colon | 0.21 ± 0.04 | 0.14 ± 0.05 | 0.14 ± 0.05 |
| Duodenum | 2.41 ± 2.45 | 2.63 ± 0.62 | 1.01 ± 0.71 |
| Fat | 1.69 ± 0.67 | 1.62 ± 0.92 | 1.03 ± 0.57 |
| Heart | 0.34 ± 0.15 | 0.14 ± 0.01‡ | 0.13 ± 0.03‡ |
| Ileum | 3.03 ± 4.70 | 2.07 ± 1.83 | 1.52 ± 2.32 |
| Kidney | 0.51 ± 0.11 | 0.28 ± 0.03* | 0.25 ± 0.05* |
| Liver | 0.55 ± 0.30 | 0.40 ± 0.07 | 0.38 ± 0.09 |
| Lung | 0.66 ± 0.47 | 0.19 ± 0.02 | 0.17 ± 0.04 |
| Muscle | 0.19 ± 0.07 | 0.13 ± 0.03 | 0.14 ± 0.05 |
| Pancreas | 0.51 ± 0.10 | 0.41 ± 0.06 | 0.38 ± 0.25 |
| Paw, control | 0.20 ± 0.06 | 0.17 ± 0.02 | 0.17 ± 0.07 |
| Paw, inflamed | 0.17 ± 0.04 | 0.15 ± 0.02 | 0.14 ± 0.04 |
| Spleen | 0.10 ± 0.02 | 0.07 ± 0.01 | 0.07 ± 0.02‡ |

Tissue uptake is expressed as SUV ± SD ($n = 4$). Values were analyzed using Student's $t$ test with $P$ as dual-tail probability. Significant differences between experimental groups, pretreated with either selective COX-2 inhibitor NS-398 or nonselective inhibitor indomethacin, and control group are indicated with symbols *$P <$ 0.01, †$P < 0.0001$, and ‡$P < 0.05$.

### Peroxidase Assay

The lack of specific binding in the inflamed paw prompted us to assess the COX enzyme activity in the inflamed paw and in a selected number of other tissues. Enzyme activity was determined by a peroxidase assay, which monitored the COX-catalyzed oxidation of TMPD with hydrogen peroxide (*19*). As depicted in Figure 4, no significant difference in COX activity was observed between the inflamed paw ($0.6 \pm 0.3 \times 10^3$ units/g) and the control paw ($0.8 \pm 0.3 \times 10^3$ units/g). High COX peroxidase activity was observed in heart ($5.6 \pm 1.5 \times 10^3$ units/g), lung ($5.6 \pm 0.5 \times 10^3$ units/g), and brain ($1.7 \pm 0.7 \times 10^3$ units/g), whereas hardly any peroxidase activity was observed in liver ($0.2 \pm 0.2 \times 10^3$ units/g). Although kidneys are known to constitutively express high levels of COX-2 (*20*), the peroxidase activity observed in the kidneys of untreated rats was surprisingly low ($0.5 \pm 0.2 \times 10^3$ units/g). However, peroxidase activity in the kidneys was significantly ($P = 0.02$) increased ($1.3 \pm 0.2 \times 10^3$ units/g) when the animals were injected with 0.3 mL of a solution of noncarrier-added compound $^{18}$F-2 in ethanol/0.9% NaCl/propylene glycol (1:2:2) 2 h before sacrifice.

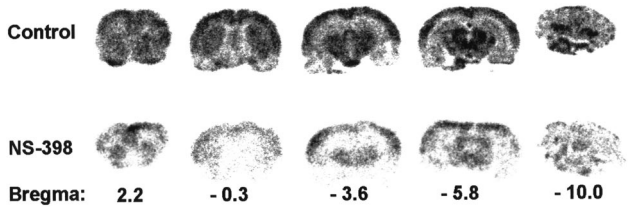


**FIGURE 3.** Phosphor images of $^{18}$F-desbromo-DuP-697 binding in coronal 80-μm-thick brain slices of untreated (top row) and NS-398 pretreated (bottom row) rats, which were killed 120 min after administration of 19 MBq of radioligand.

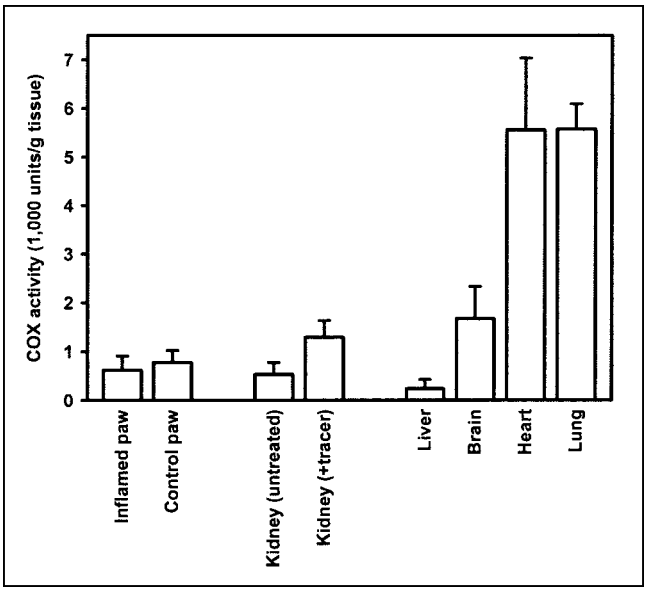


**FIGURE 4.** COX peroxidase activity in rat tissue, as assayed by COX-catalyzed oxidation of TMPD with hydrogen peroxide ($n = 4$).

## DISCUSSION

Enhanced COX-2 expression is associated with several physiologic and pathologic processes, including carcinogenesis, ischemia, angiogenesis, and neurodegeneration. A noninvasive method to monitor COX-2 expression repetitively would provide an opportunity to study the role of COX-2 in living subjects. The aim of our research was to develop a radiotracer for imaging of COX-2 expression with PET. For this purpose, a noncarrier-added radiosynthesis of the selective COX-2 inhibitor $^{18}$F-desbromo-DuP-697 (compound $^{18}$F-2) was developed. The radiolabeled COX-2 inhibitor was synthesized by a nucleophilic aromatic substitution of the nitro precursor (compound 4) with $^{18}$F-fluoride. Compound 4 is only weakly activated by electron-withdrawing substituents that facilitate the aromatic nucleophilic substitution reaction. Consequently, the labeling of desbromo-DuP-697 only proceeded at high temperatures. In spite of the poor reactivity of compound 4, sufficient amounts of compound $^{18}$F-2 can be obtained for preclinical and clinical studies.

Preclinical evaluation studies of compound $^{18}$F-2 were performed in a carrageenan-induced hyperalgesia rat model. In this model, sterile inflammation is evoked in the rat's paw by injection of carrageenan. All animals treated with carrageenan showed an increase in paw volume to approximately 150% of its original size, because of extensive edema formation. Literature data indicate that the edema formation in the inflamed paw is accompanied by an approximately 8- and 12-fold increase in COX-2 protein and mRNA levels, respectively (*17*). In the biodistribution study of compound $^{18}$F-2, however, we did not find a significantly higher tracer uptake in the inflamed paw than in the contralateral paw, in spite of the observed inflammatory response after carrageenan injection. Furthermore, tracer uptake in the inflamed paw could not be blocked by COX inhibitors. This apparent lack of specific COX-2 tracer uptake in the inflamed paw might be attributed to insufficient induction of COX-2 expression by carrageenan. This hypothesis was supported by the results of the COX peroxidase assay, which showed that peroxidase activity in the inflamed paw was similar to that in the control paw. Although the carrageenan-induced upregulation of COX-2 expression may be high relative to the low basal COX-2 levels in the paw, apparently the absolute quantities of COX-2 enzyme that are produced are still small and, therefore, could not be detected with compound $^{18}$F-2 or the peroxidase assay.

In contrast, the biodistribution studies in rats demonstrated specific binding of compound $^{18}$F-2 in brain, kidney, heart, and the cellular blood fraction. Brain and kidney are known to constitutively express basal levels of COX-2 (*21*). Okamoto and Hino showed in Fisher-344 and Brown Norway rats that substantial amounts of COX-2 mRNA were also expressed in the heart, whereas COX-1 expression could not be detected in this organ (*20*). The specific binding in the cellular fraction of the blood can be ascribed to upregulation of COX-2 expression in leukocytes, which is induced by inflammatory stimuli from the carrageenan-treated paw (*22*). The significant reduction of tracer uptake in the spleen after pretreatment with indomethacin probably reflects the specific binding to COX-2 in leukocytes in the blood reservoir of this organ. The largest decrease (70%–75%) in tracer accumulation on administration of the COX inhibitors was found in the lung. This reduction, however, was not statistically significant ($P = 0.08$), mainly as a result of the wide variation in the tracer uptake in the lungs of untreated rats. This may be due to variable COX-2 expression in the lung, as was observed by Okamoto and Hino, who could detect COX-2 in the lung of only 2 of 3 animals. Taken together, these results suggest that the tracer selectively binds to COX-2 and not to COX-1, because specific binding is only observed in tissues known to express COX-2 and because the nonselective COX inhibitor indomethacin had an effect on the biodistribution of compound $^{18}$F-2 similar to that of the selective COX-2 inhibitor NS-398.

The biodistribution data are supported by the results of the COX peroxidase assay, which revealed high levels of COX enzyme activity in lung, heart, and brain, but not in kidney. This apparent discrepancy between the low level of COX peroxidase activity and the specific tracer uptake in the kidney was the result of differences in kidney COX-2 expression between the experimental groups. Studies in Sprague–Dawley rats have shown that COX-2 expression in the renal medulla is stimulated by hypertonicity caused by dehydration (*23*). In this study, hypertonicity could have been induced by the anesthetic, because it was shown that medetomidine has diuretic properties and increases serum osmolality (*24*). Differences in the duration of the anesthesia might be responsible for differences in COX-2 expres-

sion between the experimental groups, because animals in the distribution study were anesthetized for 3 h, but animals used for the peroxidase assay were anesthetized only for 1 h. An alternative explanation could be that animals that were used in the biodistribution study had the tracer injected in 0.3 mL of cocktail of ethanol/0.9% NaCl/propylene glycol (1:2:2). The high alcohol and propylene glycol concentrations in this cocktail may have caused hypertonicity and thus induced COX-2 expression in the kidney. Animals that were used for the COX peroxidase assay did not receive any cocktail. To confirm this theory, kidney from animals that were injected with the tracer dissolved in ethanol/NaCl/propylene glycol cocktail was analyzed in the peroxidase assay. Significantly higher (2.4 times; $P = 0.02$) COX peroxidase levels were found in the kidney of animals that had received the tracer solution compared with the kidney of untreated animals (Fig. 4).

Although our results demonstrate that specific binding of compound $^{18}$F-2 to the active site of the COX-2 enzyme can be measured in organs with high levels of COX-2 expression, the tracer also showed substantial nonspecific uptake, especially in fat and in the intestines. The high uptake in fat can be ascribed to the lipophilic character of the tracer ($\log P = 3.72 \pm 0.16$), whereas the high tracer contents in the intestines were probably the result of biliary excretion. This nonspecific uptake could hamper imaging of COX-2 expression with compound $^{18}$F-2 in the abdominal region. On the other hand, the lipophilicity of compound $^{18}$F-2 allows it to pass the blood–brain barrier. Autoradiography showed that $^{18}$F-desbromo-DuP-697 was not uniformly distributed in the brain. Whether the observed tracer distribution actually correlates with the COX-2 enzyme distribution still needs to be investigated. Little is known about the regional distribution of COX-2 protein in the intact rat brain in the carrageenan-induced hyperalgesia model. Recently, it was shown that injection of carrageenan in the paw time-dependently induces high levels of COX-2 expression in the spinal cord (*25*). It is unclear if COX-2 expression in the brain is altered as well. Approximately 40% of the tracer uptake in the brain of normal rats could be blocked by the selective COX-2 inhibitor NS-398, indicating that 40% of the tracer is specifically bound to COX-2. This signal-to-noise ratio could be sufficient to study neurologic disorders. In human brain affected by Alzheimer's disease, for example, COX-2 protein levels are approximately 80% increased as compared with control brain (*7*). Thus, imaging of COX-2 expression in the central nervous system with $^{18}$F-desbromo-DuP-697 and PET appears be feasible and could be a valuable tool for studying the role of COX-2 in neurodegenerative disorders.

## CONCLUSION

The selective COX-2 inhibitor desbromo-DuP-697 was labeled with $^{18}$F in yields that are sufficient for animal and human studies. The in vivo evaluation studies showed specific binding of $^{18}$F-desbromo-DuP-697 to COX-2 in organs with known high levels of the enzyme, whereas specific binding of the tracer to COX-1 appears negligible. Nonspecific uptake of $^{18}$F-desbromo-DuP-697 in intestines and fat is high, which precludes COX-2 imaging in the abdominal region. The lipophilic character of the tracer, however, allows it to cross the blood–brain barrier, enabling COX-2 imaging in the brain. Thus, $^{18}$F-desbromo-DuP-697 could be a suitable tracer for imaging of COX-2 expression especially in the central nervous system.

## REFERENCES


1. Crofford LJ. Clinical experience with specific COX-2 inhibitors in arthritis. *Curr Pharm Des.* 2000;6:1725–1736.
2. Katori M, Majima M. Cyclooxygenase-2: its rich diversity of roles and possible application of its selective inhibitors. *Inflamm Res.* 2000;49:367–392.
3. Moran EM. Epidemiological and clinical aspects of nonsteroidal anti-inflammatory drugs and cancer risks. *J Environ Pathol Toxicol Oncol.* 2002;21:193–201.
4. Fosslien E. Molecular pathology of cyclooxygenase-2 in neoplasia. *Ann Clin Lab Sci.* 2000;30:3–21.
5. Nogawa S, Zhang F, Ross ME, Iadecola C. Cyclo-oxygenase-2 gene expression in neurons contributes to ischemic brain damage. *J Neurosci.* 1997;17:2746–2755.
6. Shinmura K, Tang XL, Wang Y, et al. Cyclooxygenase-2 mediates the cardioprotective effects of the late phase of ischemic preconditioning in conscious rabbits. *Proc Natl Acad Sci USA.* 2000;97:10197–10202.
7. Yermakova A, O'Banion MK. Cyclooxygenases in the central nervous system: implications for treatment of neurological disorders. *Curr Pharm Des.* 2000;6:1755–1776.
8. Learn CA, Mizel SB, McCall CE. mRNA and protein stability regulate the differential expression of pro- and anti-inflammatory genes in endotoxin-tolerant THP-1 cells. *J Biol Chem.* 2000;275:12185–12193.
9. Lukiw WJ, Bazan NG. Cyclooxygenase 2 RNA message abundance, stability, and hypervariability in sporadic Alzheimer neocortex. *J Neurosci Res.* 1997;50:937–945.
10. Pairet M, van Ryn J. Experimental models used to investigate the differential inhibition of cyclooxygenase-1 and cyclooxygenase-2 by non-steroidal anti-inflammatory drugs. *Inflamm Res.* 1998;47(suppl 2):S93–S101.
11. McCarthy TJ, Sheriff AU, Graneto MJ, Talley JJ, Welch MJ. Radiosynthesis, in vitro validation, and in vivo evaluation of $^{18}$F- labeled COX-1 and COX-2 inhibitors. *J Nucl Med.* 2002;43:117–124.
12. Copeland RA, Williams JM, Giannaras J, et al. Mechanism of selective inhibition of the inducible isoform of prostaglandin G/H synthase. *Proc Natl Acad Sci USA.* 1994;91:11202–11206.
13. Joshi AS, Raghavan N, Williams RM, Takahashi K, Shingu H, King SY. Simultaneous quantification of an anti-inflammatory compound (DuP 697) and a potential metabolite (X6882) in human plasma and urine by high-performance liquid chromatography. *J Chromatogr B Biomed Appl.* 1994;660:143–150.
14. de Vries EFJ, Vaalburg W. Labeling of cyclooxygenase-2 inhibitors DuP-697 and its desbromo derivative: the crucial role of the solvent. *J Labelled Cmpds Radiopharm.* 2001;44(suppl 1):S933–S935.
15. Leblanc Y, Gauthier JY, Ethier D, et al. Synthesis and biological evaluation of 2,3-diarylthiophenes as selective Cox-2 and Cox-1 inhibitors. *Bioorg Med Chem Lett.* 1995;5:2123–2128.
16. Pinto DJP, Copeland RA, Covington MB, et al. Chemistry and pharmacokinetics of diarylthiophenes and terphenyls as selective COX-2 inhibitors. *Bioorg Med Chem Lett.* 1996;6:2907–2912.
17. Nantel F, Denis D, Gordon R, et al. Distribution and regulation of cyclooxygenase-2 in carrageenan-induced inflammation. *Br J Pharmacol.* 1999;128:853–859.
18. Tsuji K, Nakamura K, Ogino T, et al. Studies on anti-inflammatory agents. VI. synthesis and pharmacological properties of 2,3-diarylthiophenes. *Chem Pharm Bull (Tokyo).* 1998;46:279–286.
19. van der Ouderaa FJ, Buytenhek M. Purification of PGH synthase from sheep vesicular glands. *Methods Enzymol.* 1982;86:60–68.
20. Okamoto T, Hino O. Expression of cyclooxygenase-1 and -2 mRNA in rat tissues: tissue-specific difference in the expression of the basal level of mRNA. *Int J Mol Med.* 2000;6:455–457.
21. Kam PCA, See AUL. Cyclo-oxygenase isoenzymes: physiological and pharmacological role. *Anaesthesia.* 2000;55:442–449.

22. Maloney CG, Kutchera WA, Albertine KH, McIntyre TM, Prescott SM, Zimmerman GA. Inflammatory agonists induce cyclooxygenase type 2 expression by human neutrophils. *J Immunol.* 1998;160:1402–1410.
23. Yang T, Schnermann JB, Briggs JP. Regulation of cyclooxygenase-2 expression in renal medulla by tonicity in vivo and in vitro. *Am J Physiol.* 1999;277:F1–F9.
24. Burton S, Lemke KA, Ihle SL, Mackenzie AL. Effects of medetomidine on serum osmolality; urine volume, osmolality and pH; free water clearance; and fractional clearance of sodium, chloride, potassium, and glucose in dogs. *Am J Vet Res.* 1998;59:756–761.
25. Doi Y, Minami T, Nishizawa M, Mabuchi T, Mori H, Ito S. Central nociceptive role of prostacyclin (IP) receptor induced by peripheral inflammation. *Neuroreport.* 2002;13:93–96.